

Gravitational Fragmentation in Galaxy Mergers: A Stability Criterion.

Andrés Escala, Fernando Becerra, Luciano del Valle and Esteban Castillo

Departamento de Astronomía, Universidad de Chile, Casilla 36-D, Santiago, Chile.

ABSTRACT

We study the gravitational stability of gaseous streams in the complex environment of a galaxy merger, because mergers are known to be places of ongoing massive cluster formation and bursts of star formation. We find an analytic stability parameter for case of gaseous streams orbiting around the merger remnant. We test our stability criteria using hydrodynamic simulations of galaxy mergers, obtaining satisfactory results. We find that our criterion successfully predicts the streams that will be gravitationally unstable to fragment into clumps.

Subject headings: instabilities - galaxies: interactions - galaxies: formation - galaxies: star clusters: general

1. Introduction

Galaxy mergers are believed to be not just common events in the universe, but also fundamental pieces in the evolution of galaxies since they trigger bursts of star formation (Larson & Tinsley 1978; Sanders & Mirabel 1996) and they are a key ingredient in the formation Elliptical Galaxies and Bulges (Toomre & Toomre 1972; Mihos & Hernquist 1994, 1996; Kazantzidis et al. 2005; Di Matteo et al. 2007). More recently, it was also found that many interacting and merging galaxies are places of current massive cluster formation (Schweizer 1998; Mengel et al. 2008).

Standard numerical simulations of galaxy mergers that include gas (Mihos & Hernquist 1994; Barnes & Hernquist 1996; Kazantzidis et al. 2005; Cox et al. 2006; Di Matteo et al. 2007), have been able to reproduce the observed starbursts occurred during the merging process on nuclear gaseous disks. However, they intentionally avoid fragmentation through high minimum temperatures and large gravitational softening lengths, therefore, they failed to reproduce formation of massive star clusters. Only recently, simulations have the resolution required to study the gas fragmentation on at least large scales (Bournaud et al. 2008; Saitoh et al. 2009; Teyssier et al. 2010; Matsui et al 2012). In those simulations, massive

star clusters are indeed formed by gas fragmentation into collapsing clumps and therefore is relevant to have a criteria for gravitational instabilities in such complex environment.

The study of gravitational stability of fluids started with the work of Jeans (1902) for a uniform, infinite and isothermal gas. Later extended by Bonnor (1956) and Ebert (1955) for a finite and spherically symmetric fluid, a rotationally supported one (Toomre 1964; Goldreich & Lynden Bell 1965), a magnetized fluid (Chandrasekhar & Fermi 1953), among others. In this letter, we study the stability of the gaseous streams in the complex environment of a galaxy merger, by means of Smoothed Particle Hydrodynamics (SPH) numerical simulations.

This work is organized as follows. We start with a discussion of the physical processes relevant in stabilizing gaseous streams in galaxy mergers, with analytical estimates for a stability criterion in §2. Section 3 continues discussing the setup of the galaxy mergers simulations and the resolution needed to resolve gravitational instabilities in galaxy mergers. In §4, we test the stability criteria by performing hydrodynamical simulations of galaxy mergers with the resolution discussed in §3. Finally in §5, we summarize the results of this work.

2. Basic Physical Ingredients: Gas Pressure and Motion

High-resolution simulations of galaxy mergers generally found galactic streams, such as tails and bridges at large scales and more complex ones on the inner kpc scales, in which collapsing clumps are ubiquitous features formed by gravitational instabilities. However, no gravitational instability criterion for the complex and irregular case of gaseous streams in a galaxy merger has been found.

The most basic physical processes that could overcome gravity in absence of magnetic and other fields are gas pressure and motion. Since gas pressure is isotropic, does not depend on the geometry of the fluid, only on its local density and temperature, therefore its stabilizing role on small scales is the same that in a fluid with a regular geometry (i.e with a given symmetry). On the other hand, the motion of streams is much more complex and not constrained to a single plane, but on its central regions (inner kpc, where the bulk of the star and cluster formation happens) is characterized by streams orbiting around the center of mass of the newly formed system.

A simple and useful approach is to model individual streams as a piece of a rotating annulus. In such a case, from vector calculus is known that the rotational component of its motion is well described by an angular frequency, which is defined relative to an origin O of

the coordinate system in which we describe the motion:

$$\vec{\Omega}_o = \frac{\vec{r} \times \vec{v}}{\vec{r} \cdot \vec{r}} = \frac{\vec{r} \times \vec{v}}{r^2} = \hat{r} \times \frac{\vec{v}}{r} , \quad (1)$$

where $\vec{r} = r \hat{r}$ and \vec{v} are, respectively, the position and velocity vectors.

Under this approximation, the stability of individual streams is a very similar problem to the stability of annuli in a rotating sheet, with the difference that the streams in the merger case do not belong to the same plane ($\vec{\Omega}_o$ of individual streams can have a different magnitude and direction). In such a case, from dimensional analysis it is straightforward to conclude that results from standard gravitational instability analysis in a rotating sheet (Toomre 1964; Goldreich & Lynden Bell 1965; Binney & Tremaine 2008) should still be valid for a given stream: there is a range of unstable length scales limited on small scales by thermal pressure (at the Jeans length $\lambda_{\text{Jeans}} = C_s^2/G\Sigma_{\text{gas}}$) and on large scales by rotation (at the critical length set by rotation, which for this case can be defined as $\lambda_{\text{rot}} \equiv \pi^2 G \Sigma_{\text{gas}} / |\vec{\Omega}_o|^2$). All intermediate length scales are unstable, the most rapidly growing mode has a wavelength $2 \lambda_{\text{Jeans}}$ and the most unstable mode has a wavelength $\lambda_{\text{rot}}/2$. Only a combination of pressure and rotation can stabilize the stream, this happens when the range of unstable wavelengths shrinks to zero (i.e. the two scales are comparable) and this occurs for $\lambda_{\text{Jeans}} \geq (q/\pi)^2 \lambda_{\text{rot}}$ (Escala & Larson 2008). Therefore a stream will be stable if:

$$|\vec{Q}_o| \equiv \frac{C_s |\vec{\Omega}_o|}{G \Sigma_{\text{gas}}} \geq q , \quad (2)$$

where C_s is the gas sound speed, $|\vec{\Omega}_o|$ is the norm of the angular frequency vector, G is the gravitational constant, Σ_{gas} is the gas surface density and q is a number of the order of unity. Otherwise, if $|\vec{Q}_o| < q$, a stream will be unstable.

It is important to point out that the concept of angular frequency depends on the origin of the coordinate system chosen to describe the motion, and contrary to the case of the rotating sheet, there is not an obvious single choice for all streams in a galaxy merger. This becomes relevant in section 4, when we compare the results of this section with numerical simulations, for testing if the stability criteria given by Eq 2 is valid or not. Our approach in section 4 will be to check if with a single origin of the coordinate system O , Eq 2 is able to predict the gravitational instability of the streams. This assumption will introduce changes in the value of the angular frequency and therefore, in the determination of the value for the threshold q (will be an average value for all streams). However, our aim is to have a simple criteria that can be easily applied by other authors and in such a case, is better to have a single $|\vec{Q}_o|$ with an average fitting parameter q , than one $|\vec{Q}_{o\alpha}|$ and q_α for each α th stream.

In the case that all the streams are coplanar and orbit around the same point, we recover the standard Toomre Q parameter for a rotating sheet ($=C_s \Omega/G \Sigma_{\text{gas}}$; Toomre 1964), since

now the direction of $\vec{\Omega}_0$ and the origin O chosen to describe the motion, is the same for all streams.

3. Simulations of gravitational fragmentation in galaxy mergers

In the following we perform a set of idealized numerical experiments aimed to test if the stability parameter (Eq. 2), successfully predicts the streams in a galaxy merger that will be gravitationally unstable to fragment into clumps. These experiments are constructed as simple as possible, in order to guarantee that the gas fragmentation is only due to gravitational instabilities. For that reason, we use an isothermal equation of state instead of having a multiphase medium and do not include any feedback processes from star formation and/or AGN which will make more complex the analysis as it includes new sources that may trigger fragmentation. Without including this extra physics we cannot aim to have a realistic description of the ISM, but will be enough for our main purpose, which is to study the onset of gravitational instability at large scales in a galaxy merger.

The simulation consists on the merger of two equal mass disk galaxies and we let the two galaxies collide in a parabolic orbit with pericentric distance $R_{\min} = 7.35$ kpc. The simulations start with an initial separation of 49 kpc, where the separation distance is measured between the mass centers of the two galaxies and the initial inclination angle between disk planes of individual galaxies is 90° . The galaxies are initialized using the code GalactICS, in particular we used their ‘Milky Way model A’ (see Kuijken & Dubinski 1995 for details). In each galaxy model, we include a gaseous disk with the same exponential profile as the stellar component (Kuijken & Dubinski 1995) and with a total gas mass corresponding to the 10% of the total stellar disk mass. The gas has an isothermal equation of state, $P = c_s^2 \rho$, where the sound speed is fixed at $c_s = 12.8 \text{ km s}^{-1}$, corresponding to a gas temperature of $\sim 2 \times 10^4 \text{ K}$. At $t=0$, the gaseous disk of each isolated galaxy is gravitationally stable. In our simulations, we use the following internal units : [Mass] = $5.8 \times 10^{11} M_\odot$, [Distance] = 1.2 kpc and $G=1$. The total number of particles is 420,000, being 200,000 for sampling the gas, 120,000 for the dark matter halo, and 80,000 for the disk component and 20,000 for the bulge.

The simulations were evolved using the SPH code Gadget-2 (Springel 2005), up to a time $t=160$ (in internal time units), which correspond to a point where the galaxies are after their third (and final) pericentric passage and in which most of the gas ($> 80\%$) has been fueled to the central kpc. Fig 1 (a, b, c, d) show the evolution of the system at four times $t = 32$ (a), 54 (b), 120 (c) and 136 (d) which corresponds to before (a) and after (b) the first pericentric passage, second pericentric passage (c) and in their third pericentric encounter (d). The ring/oval structures seen on Fig. 1(a, b, c), are ubiquitous features since early

simulations of galaxy mergers (e.g., Schwarz 1984) and are believed to be tightly wound spirals that are the gas response to tidal forcing (e.g., Barnes & Hernquist 1996).

3.1. Minimum Gravitational Resolution

Before analyzing the stability of gaseous streams it is necessary to check that we have the gravitational resolution required to resolve the fragmentation of streams into collapsing clumps, for that reason we performed a convergence test. We restarted the original simulation with a gravitational softening length $\epsilon_{\text{soft}}=0.4$ at $t=132$, with the following gravitational softening ϵ_{soft} : 0.04, 0.02, 0.01, 0.008, 0.006 in internal units.

Fig 1 (e, f, g, h) shows the evolution of the restarted simulation at a later time $t=134$, in a region of radius 2 internal distance units (2.4 kpc) for different gravitational softening lengths: 0.4(e), 0.04(f), 0.01(g), 0.006(h). Fig 1 (e, f, g, h) shows that as the softening lengths decrease, we find more gas fragmentation until a point in which the resulting simulations converge. We find convergence of the results for $\epsilon_{\text{soft}} \leq 0.01$ and for that reason, we choose to use in the following section a gravitational softening length of $\epsilon_{\text{soft}} = 0.01$.

The convergence can be understood if we take into account that over 99.6% of the particles in such region fulfill the condition $\lambda_{\text{rot}} \geq 4\epsilon_{\text{soft}}$ for $\epsilon_{\text{soft}} = 0.01$ and below. The convergency when λ_{rot} is resolved for all particles, is the first suggestion for supporting our definition for λ_{rot} in this environment with disordered motion ($\lambda_{\text{rot}} \equiv \pi^2 G \Sigma_{\text{gas}} / |\vec{\Omega}_o|^2$). This convergence is an evidence that the minimum requirement to resolve fragmentation at least on the largest scales, is to be able to resolve gravity below our definition for the largest unstable scale λ_{rot} .

In this set of numerical experiments, we resolve fragmentation from the largest unstable scale down to our gravitational resolution. Below the gravitational softening, sub-fragmentation is artificially damped but our aim is to study if Eq 2 can predict the instability of streams and for that purpose, is not required to resolve all the range of unstable wavelengths and is enough with the largest one, since λ_{rot} is the first unstable wavelength to appear (i.e. the most unstable mode; Binney & Tremaine 2008).

This resolution test illustrates that in a set of simulations with the same temperature, fragmentation can be prevented just by the gravitational resolution. This contradicts the interpretation of Teyssier et al. (2010), in which the onset of fragmentation is always associated with a decrease in the temperature. However, Teyssier et al. (2010) changes both temperature and resolution, being unable to disentangle which one (or both) is responsible for the onset of fragmentation. This reinforces our approach of testing the stability criteria

(Eq. 2) against a set of simple simulations, where the variation of parameters can be fully controlled.

Finally, it is worth to mention that in this section and in the rest of the paper, we will focus only in the fragmentation of the gaseous component. The reason is that the stellar component behaves approximately as an adiabatic fluid (i.e. the kinetic energy in stellar motions cannot be lost or "radiated" away from the merging system). This yields to a rapid conversion of coherent motions into random ones during the merger, with the subsequent increase of the velocity dispersion in the stellar component, stabilizing the stellar system against runaway fragmentation.

4. Test of the stability criteria $|\vec{Q}_o|$

After checking the gravitational resolution needed to resolve fragmentation at least on scales below those of the largest collapsing clumps, we will focus on testing the stability criteria discussed in §2 (Eq. 2). Since most of the streams in the inner 2.4 kpc of the system already fragments for $T \sim 2 \times 10^4 K$, we will perform a set of simulations in which we increase the temperature and see how some streams become stable. We will check if the criteria given by Eq 2, successfully predicts if a stream should be stable or not.

Fig 2 (a, b, c) shows the evolution of the gas density for the system restarted with a gravitational softening length of $\epsilon_{\text{soft}} = 0.01$, at $t=132$, for different temperatures $T=2 \times 10^4$ (a), 2×10^5 (b) and $10^6 K$ (c) and evolved to a later time $t=133.2$. The comparison between different temperatures (a to c in Fig 2) clearly shows that more streams become stable as we increase the temperature.

Fig 2 (d, e, f) shows $|\vec{Q}_o|/q$ computed for each particle at the time in which all the simulations were restarted with $\epsilon_{\text{soft}} = 0.01$ ($t= 132$), for different temperature $T=2 \times 10^4$ (d), 2×10^5 (e) and $10^6 K$ (f). For computing \vec{Q}_o , we choose as origin O of the coordinate system the total center of mass (G) of the merging galaxies, because the system as a whole orbits around G and is also an inertial point for an isolated merger (in absence of external forces). From Eq. 2, the threshold for stability should be around $|\vec{Q}_o|/q = 1$, which corresponds to the yellow particles in the figure 2, the green and blue particles should be unstable and the red ones stable.

The direct comparison of two sides of Fig 2 (a-d, b-e and c-f pairs), shows overall a good agreement between the predicted unstable streams (showed in green and blue in Fig 2 (d, e, f)) and the streams that eventually fragments on the corresponding Fig 2 (a, b, c). In particular, the bluest stream in Fig 2 d (and in light green in Fig 2 f) is the most unstable

region and the only one that strongly fragments in all simulations (including Fig 2 c) besides the increase in temperature up to 10^6 K.

We find that the stability of gaseous streams is better described for a threshold value $q \sim 0.4$, in fact, we plot $|\vec{Q}_o|/0.4$ in Fig 2 (d, e, f). This is approximately a factor of 2 lower than the value expected for a uniformly rotating isothermal disk ($q = 1.06$; Goldreich & Lynden-Bell 1965). However, it is important to emphasize that the actual value of q should depend on the origin O chosen for the coordinates system.

In order to check the numerical reliability of our results, we performed the same fragmentation runs with 2,000,000 particles for the different temperatures showed in Fig 2 (a, b, c). Fig 2 (g, h, i) shows the evolution of the gas density for the high-resolution runs. By direct comparison of two sides of Fig 2 (a-g, b-h, and c-i pairs), we found differences in the low-density regions, as expected in the SPH technique, and slightly different positions in some streams, also expected due to the different granularity of the gravitational potential. However, we found the same results in terms of the onset of fragmentation on streams (i.e. which ones fragments at a given temperature and which ones don't) and in the number of clumps formed. Therefore, for the purpose of our study, we found consistent results between the low and high resolution runs. This supports the reliability of our numerical experiments that tests Eq. 2.

Finally, it is important to note that although we successfully tested Eq. 2 for $t=132$, it should be valid at any given time for the value of the angular velocity vector in such moment (only with small variations on the threshold q). This is particularly important because, during the evolution of a galaxy merger, the properties of any stream (angular frequency vector, surface density, etc.) can drastically change on a timescale comparable to a crossing time. To check that our criteria is valid at any time, we restarted the original low-resolution simulation again at a different time $t=137.2$, with a gravitational softening $\epsilon_{\text{soft}} = 0.01$ and a temperature $T=2 \times 10^4$ K.

Fig 3a shows the evolution of the gas density for the system restarted at $t=137.2$ and evolved to a later time $t=138.4$. Fig 3b shows $|\vec{Q}_o|/q$ computed for each particle at the time $t=137.2$ using the same previously used threshold value $q=0.4$. The direct comparison of two sides of Fig 3, shows again an overall good agreement between the predicted unstable streams (showed in green and blue in Fig 3b) and the streams that eventually fragments in the evolution of the SPH run (Fig 3a).

Although the gas properties (and predicted $|\vec{Q}_o|$) in this second restarting time has considerably changed compared to the properties in the original ones (Fig 2), Fig 3 shows that the $|\vec{Q}_o|$ computed at the restarting time $t=137.2$, successfully predicts which streams

will fragment and which ones don't. This is besides some minor discrepancies that may arise if we focus on some small scale features showed in Fig 3. For example, a careful inspection of Fig 3a shows a smooth spiral pattern around a big clump (slightly up from the center of the image). On the corresponding Fig 3b, both features are in blue ($|\vec{Q}_o|/q \ll 1$) which is expected for the big clump but not for the smooth spiral feature.

Fig 4 shows a zoom-in of such region, in which the left panel shows the gas density and the right panel the corresponding $|\vec{Q}_o|/q$. From Fig 4 is straightforward to realize that the spiral is composed by only few tens of particles that were lost within the several thousands of particles that compose a clump (i.e. less than 1%). These particles, were probably lost thru the interactions with other clumps and in fact the spiral pattern ends on the closest collapsed clump, suggesting that are particles lost during strong gravitational interactions between the clumps. These minor discrepancies are inherent of the complexity of the problem, because processes that happens on the subsequent evolution, such as clump-clump interactions, are of course not included on this or any stability criterion.

In order to quantify these minor discrepancies, we plot in Fig. 5 the surface density of each particle against $|\vec{Q}_o|/q$. The left panel of Fig. 5, shows the surface density at the restarting time $t=132$ against $|\vec{Q}_o|/q$ computed at the same time. The dashed line represents $\Sigma_{\text{gas}} \propto (|\vec{Q}_o|/q)^{-1}$, which is the overall trend of particles at the restarting time. This is expected from the definition given by Eq 2, taking into account that C_S is constant and that the dispersion from the overall trend, is due to variations of $|\vec{\Omega}_o|$ among particles.

The middle and right panels of Fig. 5, shows the surface density at the $t=133$ (middle) and 134 (right) against $|\vec{Q}_o|/q$ computed at the restarting time $t=132$. By construction, the particles on middle and right panels of Fig. 5 can only move in the vertical direction (relative to their position in the left panel) and therefore it will inherently introduce scatter into the $\Sigma_{\text{gas}} \propto (|\vec{Q}_o|/q)^{-1}$ trend, since the surface density and $|\vec{Q}_o|/q$ are computed at two different times. Beside the increase in scatter, we see a coherent vertical change for $|\vec{Q}_o|/q \leq 1$ as the collapse proceeds. For isothermal simulations like the ones carried out in this work, once the gravitational instability is started it will proceed until the particles reach separations comparable to the softening length and this behaviour happens regardless the $|\vec{Q}_o|/q$ or Σ_{gas} values. The horizontal saturated region on middle and right panels of Fig. 5 (at $\log(\Sigma_{\text{gas}}) \geq 0$) denotes this behaviour. On the other hand, the time to move to the saturated region (free fall time) it does depends on Σ_{gas} and this explains why dark region of particles with $\log(\Sigma_{\text{gas}}) \leq 0$ recedes towards higher $|\vec{Q}_o|/q$ as times evolves (from $\log(|\vec{Q}_o|/q) \geq -1.5$ in the middle panel to $\log(|\vec{Q}_o|/q) \geq -1$ in right panel of Fig. 5).

In the right panel of Fig. 5, the particles in the region $\log(\Sigma_{\text{gas}}) \leq 0$ and $\log(|\vec{Q}_o|/q) \leq -1$, are representative of particles lost from the collapsing clumps, like the ones showed in

the spiral feature of Fig. 4. In the same way, the particles in the region $\log(\Sigma_{\text{gas}}) \geq 0$ and $\log(|\vec{Q}_o|/q) \geq 0$, represents particles from stable regions that are gravitationally captured by the collapsing clumps. Besides these departures, the overall trend is clear and is showed in the right panel of Fig. 5, where a drastic change at $\log(|\vec{Q}_o|/q) = 0$ is clearly seen and that is due to the collapse of the unstable regions, which moves their particles vertically up, producing the vertical saturated region seen for $\log(|\vec{Q}_o|/q) \leq 0$.

5. Summary

In this paper, we have studied the gravitational stability of gaseous streams in the complex environment of a galaxy merger, using hydrodynamic simulations.

We find that the standard Toomre Q stability parameter can be generalized for case of gaseous streams orbiting around the merger remnant, by using the angular frequency vector of each stream. This is valid as long as the orbital motion of a stream can be well approximated by the rotational motion around the center of gravity on a given plane, which is what happens in the inner regions of the merger remnant.

We test our generalized stability criteria, $|\vec{Q}_o| \geq q$, using SPH numerical simulations specially designed for that purpose. We find that this criteria successfully predicts the streams that will be gravitationally unstable to fragment into clumps. We find that the stability of streams is better described choosing a threshold value $q \sim 0.4$.

The generalization of λ_{rot} in a galaxy merger, is also relevant for the formation of massive globular-type clusters since its associated mass $M_{\text{rot}} = \Sigma_{\text{gas}} (\lambda_{\text{rot}}/2)^2$, is related to the characteristic mass of the most massive clusters that are able to form (Escala & Larson 2008; Shapiro et al. 2010) and has a role in the triggering of star formation, since it correlates with the galactic star formation rate (Escala 2011).

The numerical validation of stability for $|\vec{Q}_o| \geq q$ opens new possibilities for future research. One is to apply the criterion given by Eq. 2 to observations of gas-rich galaxy mergers and also, to simulations with a more realistic description for the ISM, that includes feedback processes from star formation and/or AGN. Another interesting possibility is to study when in the evolution of a merger, you have a larger portion of the gaseous mass with $|\vec{Q}_o| \leq q$ and then be able to determine when the streams would fragment more vigorously.

A.E. acknowledges partial support from the Center for Astrophysics and Associated Technologies CATA (PFB 06), FONDECYT Iniciacion Grant 11090216. F.B. and L. del V. acknowledge support from Programa Nacional de Becas de Posgrado (Grant D-22100632

and Grant D-21090518). The simulations were performed using the HPC clusters Markarian (FONDECYT 11090216), Geryon (PFB 06) and Levque.

REFERENCES

- Barnes, J. E.; Hernquist, L., 1996, *ApJ*, 471, 115
- Binney, J., Tremaine, S. 2008, *Galactic Dynamics*. Princeton University Press, Princeton
- Bonnor, W. B., 1956, *MNRAS*, 116, 351
- Bournaud, F. et al., 2008, *MNRAS*, 389, 8
- Chandrasekhar, S., Fermi, E., 1953, *ApJ*, 118, 116
- Cox T. J. et al., 2006, *ApJ*, 650, 791
- Di Matteo, P et al., 2007, *A&A*, 468, 61
- Ebert, R., 1955, *ZA*, 37, 217
- Escala A., Larson R. B., 2008, *ApJ*, 685, L31
- Escala, A., 2011, *ApJ*, 735, 56
- Goldreich, P., Lynden-Bell, D., 1965, *MNRAS*, 130, 97
- Jeans, J. H., 1902, *RSPTA*, 199, 1
- Kazantzidis, S. et al., 2005, *ApJ*, 623, 67
- Kuijken, K., Dubinski, J., 1995, *MNRAS*, 277, 1341
- Larson R. B., Tinsley B. M., 1978, *ApJ*, 219, 46
- Matsui, H., et al., 2012, *ApJ*, 746, 26
- Mengel, S. et al, 2008, *A&A*, 489, 1091
- Mihos, J. C., Hernquist, L., 1994, *ApJ*, 431, 9
- Mihos, J. C., Hernquist, L., 1996, *ApJ*, 464, 641
- Saitoh, T. et al., 2009, *ASJ*, 61, 481

Sanders D. B., Mirabel I. F., 1996, *ARA&A*, 34, 749

Schweizer, F., Seitzer, P., 1998, *AJ*, 116, 2206

Shapiro, K. L. et al., 2010, *MNRAS*, 403L, 36

Springel, V., 2005, *MNRAS*, 364, 1105

Teyssier, R. et al., 2010, *ApJ*, 720, 149

Toomre, A., 1964, *ApJ*, 139, 1217

Toomre, A., Toomre, J., 1972, *ApJ*, 178, 623

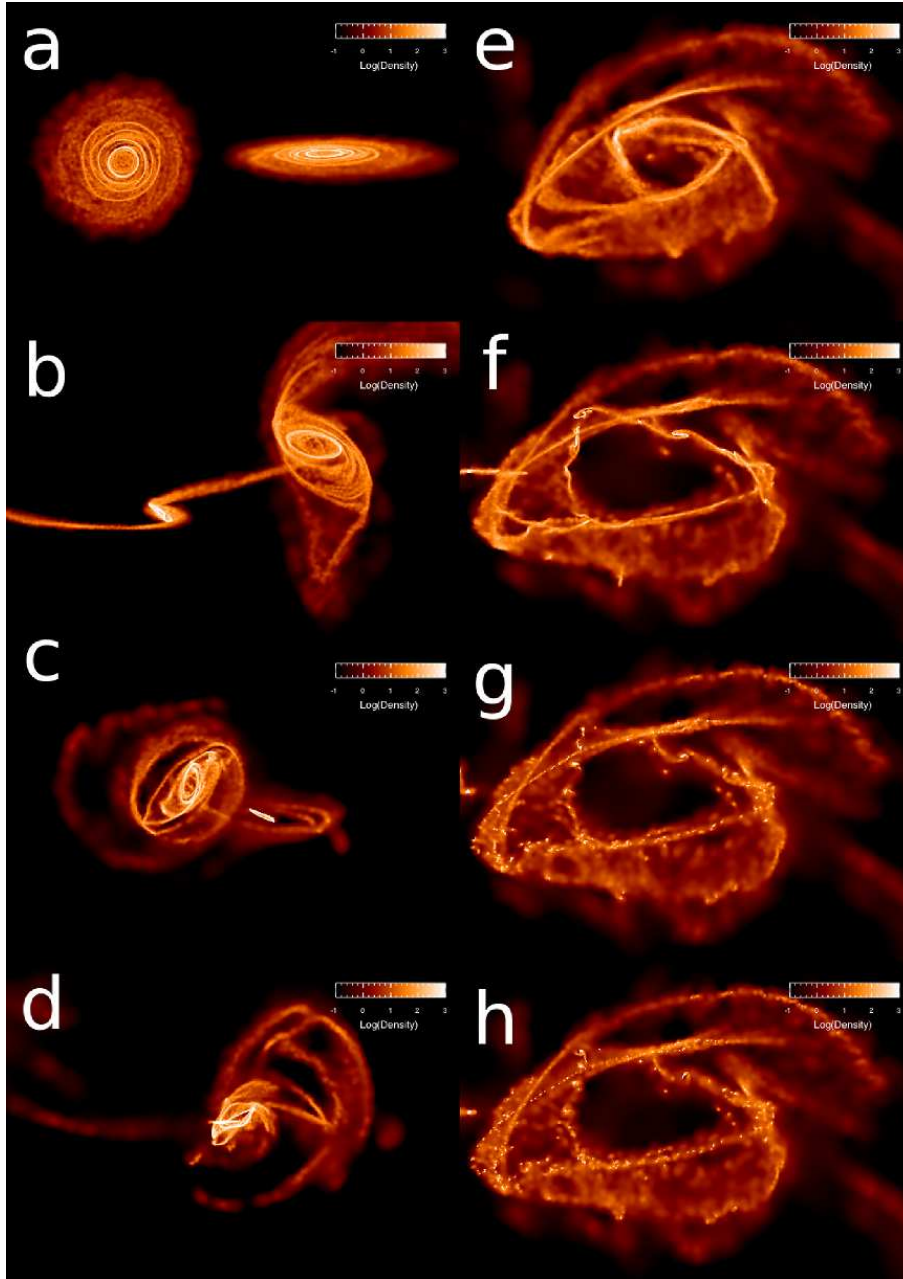


Fig. 1.— Gas density distribution during the evolution of the galaxy merger showed in a logarithmic scale. Left side panels in the figure show the density distribution in a box of side 25, in internal units, at the following times $t = 32$ (a), 54 (b), 120 (c) and 136 (d). Right side panels show a zoom in of the simulation restarted at $t=132$ (box of side 4 in internal distance units), evolved up to time $t=134$ using the following gravitational softening lengths: 0.4(e), 0.04(f), 0.01(g), 0.006(h).

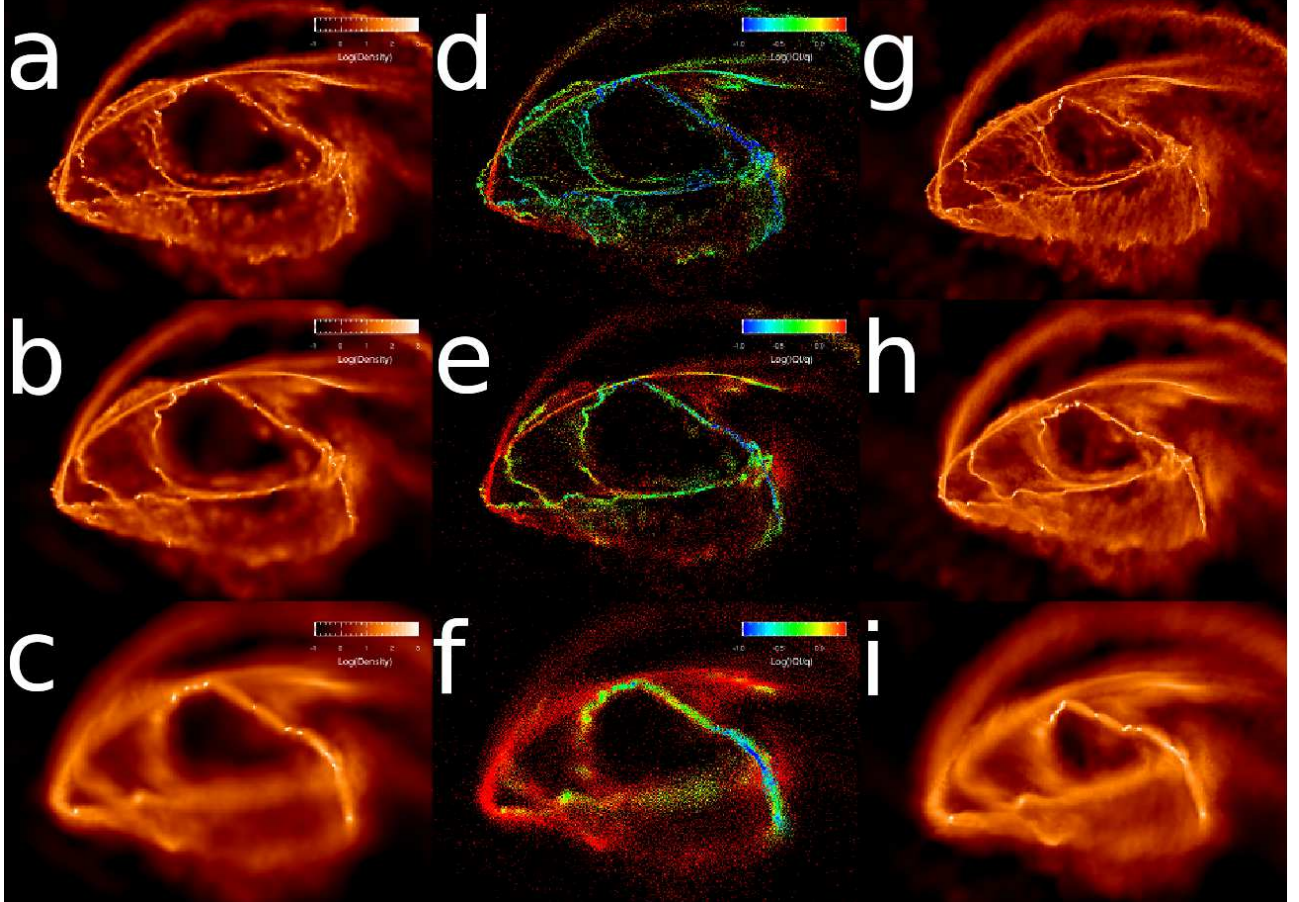


Fig. 2.— Left side panels show the evolution of the gas density distribution at $t=133.2$, for different temperatures $T=2 \times 10^4$ (a), 2×10^5 (b) and 10^6 K(c). Middle panels show the predicted $|\vec{Q}_0|/q$ for each particle, which is computed at the restarting time $t=132$, for the following temperatures $T=2 \times 10^4$ (d), 2×10^5 (e) and 10^6 K(f). Right side panels show the evolution of the gas density in the high resolution runs, for different temperatures $T=2 \times 10^4$ (g), 2×10^5 (h) and 10^6 K(i). In all figures, the boxes have a side of 4 internal distance units.

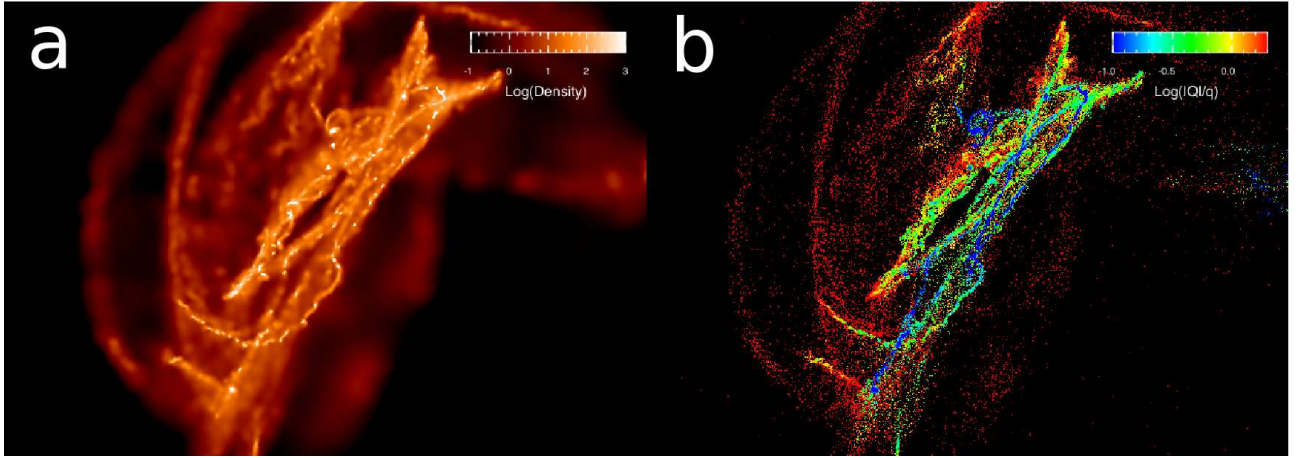


Fig. 3.— a) The gas density distribution at $t=138.4$ of a simulation with a temperature $T=2 \times 10^4$ K, that was restarted at $t=137.2$ with a gravitational softening $\epsilon_{\text{soft}} = 0.01$. b) The predicted $|\vec{Q}_o|/q$ for each particle, which is computed at the restarting time $t=137.2$, for a temperature $T=2 \times 10^4$ K.



Fig. 4.— Zoom into the simulation showed in figure 3. Left: The gas density for each particle at $t=138.4$. Right: The predicted $|\vec{Q}_o|/q$ for each particle, which is computed at the restarting time $t=137.2$

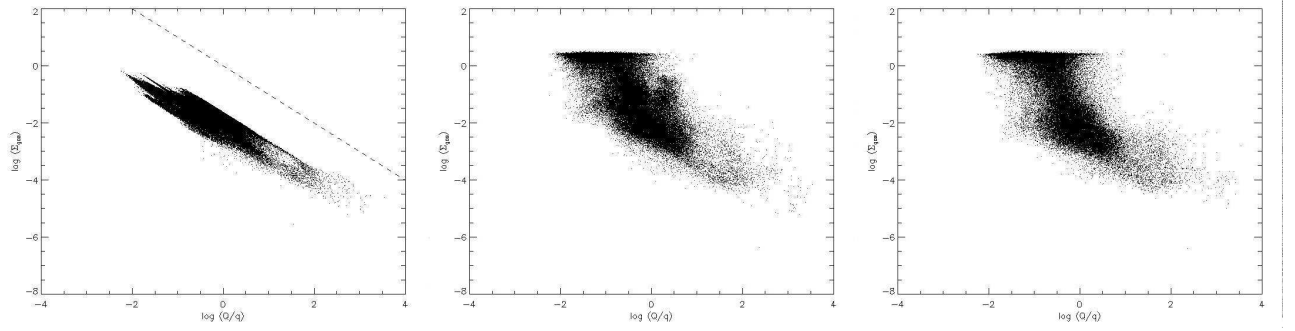


Fig. 5.— Evolution of the surface density as fragmentation proceeds. The predicted $|\vec{Q}_0|/q$ for each SPH particle, which is computed at the restarting time $t= 132$, plotted against the surface density of each particle at a time $t= 132$ (right), 133 (middle) and 134 (left).